Fibrous Long-Chain Organic Acid Cellulose Esters and Their Characterization by Diffuse Reflectance FTIR Spectroscopy, Solid-State CP/MAS ^{13}C-NMR, and X-Ray Diffraction

PETER JANDURA,[1] BOHUSLAV V. KOKTA,[1] BERNARD RIEDL[2]

[1] Pulp and Paper Research Center, University of Quebec, C.P. 500, Trois-Rivières, Quebec, Canada G9A 5H7

[2] Center for Research on Science and Engineering of Macromolecules, Wood Science, Faculty of Forestry, Laval University, Quebec, Canada G1K 7P4

Received 15 November 1999; accepted 30 March 2000

ABSTRACT: Unsaturated and saturated organic acids with 11 and 18 carbon atoms, respectively, were used in a heterogeneous esterification reaction in the pyridine/toluene sulfonyl chloride system to prepare fibrous cellulose esters with different degrees of substitution. Highly bleached sulfite cellulose fibers were esterified during a 1- or 2-h reaction time with the following organic acids: undecylenic acid, undecanoic acid, oleic acid, and stearic acid. In all cases, the heterogeneous esterification yielded partially substituted cellulose esters retaining their fibrous structure. The substitution reaction was confirmed by diffuse reflectance infrared spectroscopy and the chemical structures of cellulose esters were identified by solid-state CP/MAS ^{13}C-NMR (75.3 MHz). X-ray diffraction analyses showed broadening of the diffraction peaks with a higher degree of substitution of cellulose esters, which suggests structural changes within the cellulose fibers. Because the broadening peaks of X-ray spectra or the unassigned C-4 region of substituted cellulose chains in NMR spectra do not allow the calculation of dimensional changes of cellulose crystallites in cellulose esters, the lateral dimensions of crystallites in only cellulose fibers were calculated. The value derived from NMR (4.6 nm) differs by about 11% when compared with the value calculated from X-ray diffraction data (4.1 nm). J Appl Polym Sci 78: 1354–1365, 2000

Key words: long-chain organic acid cellulose esters; undecylenic acid; undecanoic acid; oleic acid; stearic acid; FTIR–DRIFT; ^{13}C-NMR; X-ray diffraction

INTRODUCTION

Acetylation is the most widely used esterification reaction on cellulose and has had an industrial use for a long time. When the reaction of acetic anhydride in the presence of glacial acetic acid with a sulfuric acid catalyst proceeds to a higher degree of substitution, the primary structure of cellulose is lost and the substituted cellulose chains are organized into two polymorphic forms analogous to the original cellulose I or II.[1]

Crofton et al.[2] reported small morphological changes when the solvent system used is aprotic and that the order is retained to a significant extent even in the completely substituted material. The heterogeneous nature of the chemical substitution of cellulose hydroxyl groups reflects the accessibility of the reaction site to the mole-

Correspondence to: P. Jandura.
Contract grant sponsor: Natural Science and Engineering Research Council (NSERC), Canada.

Journal of Applied Polymer Science, Vol. 78, 1354–1365 (2000)

cules of an organic acid. It has been reported that the acetylation of cellulose linters with acetic acid in an aprotic solvent, such as pyridine, does not significantly affect the crystalline regions.[3] The same observation comes from another report which described the preparation of some acyl derivatives of microcrystalline cellulose (from butyryl to stearyl) in CCl_4/heptane.[4] Doyle et al.[5] proposed that the initial acetylation in heterogeneously esterified cellulose occurs in disordered regions, which may thereafter be solubilized, but that subsequent acetylation permits the preservation of order in the sample.

There are only a few studies on heterogeneous esterification of cellulose fibers with long-chain organic acids in an aprotic solvent.[6–8] These esters are identified as potential biodegradable plastics due to the enzymatically labile ester bond and the natural abundance of both cellulose and long-chain organic acids.[9] When modified fibers are used in cellulose–polymer composites as a filler/reinforcing agent, not only chemical but also morphological changes, surface energetics, or thermal properties significantly affect their overall behavior in a polymer matrix. In this article, the preparation and characterization of such cellulose esters using infrared spectroscopy FTIR–DRIFT, solid-state CP/MAS ^{13}C-NMR, and X-ray diffraction are reported.

EXPERIMENTAL

Chemicals

Pyridine (Py), *p*-toluenesulfonyl chloride (TsCl), and all organic acids (undecylenic acid, undecanoic acid, oleic acid, stearic acid) were A.C.S. reagents supplied by Aldrich (Oakville, Ontario, Canada) and they were used without any further purification.

Cellulose Sample

The cellulose used in this work was highly purified bleached sulfite pulp (PUGET ULTRA 60/40% Radiata Pine/Western Hemlock blend) provided by the Georgia–Pacific Corp. (Bellingham, WA, USA). The sample was received in dry sheet form and the cellulose fibers were prepared for the esterification reaction following the disintegration procedure. The technical data of the cellulose sample was brightness ISO 95.1, α-cellulose content 92.5%, ash 0.23%, pH 7.0, and arithmetic fiber length 0.76 ± 0.03 mm measured after disintegration in a mixer.

Abbreviations

In the text, the following abbreviations are used: undecylenic acid (UNA), undecanoic acid (UNC), oleic acid (OLA), stearic acid (STA), pyridine (Py), *p*-toluenesulfonyl chloride (TsCl), cellulose (CEL), cellulose esters (CEL-EST), cellulose esters where organic acids with 11 or 18 carbon atoms were used in the esterification reaction (CEL-EST-11) or (CEL-EST-18), respectively; cellulose undecylenate (CEL-UNA), cellulose undecanoate (CEL-UNC), cellulose oleate (CEL-OLA), cellulose stearate (CEL-STA), and 1-h esterification reaction (A) and 2-h (B); ex. CEL-UNA-B is cellulose undecylenate synthesized after 2 h of reaction time.

Preparation of Cellulose Fibers

In the following procedure, the separate cellulose fibers were prepared from dried cellulose sheets. First, the cellulose sheet was cut by hand into small pieces and disintegrated in demineralized water in a low-speed blender for 1 h. The cellulose fibers were filtered and dried at 50°C for 3 days. After drying, a low-density bulk form of cellulose fibers was obtained. In the second stage, 15 g of cellulose fibers were placed in a mixer containing 1 L of 95% ethanol, then disintegrated for 1 min and filtered. The edges of the mixer knives were smoothly rounded to minimize cutting of the cellulose fibers. Finally, the fibers were dried through a screen by compressed air and then dried in an oven for 2 h at 70°C to remove any residual ethanol. Prepared cellulose fibers were used for analysis and in all esterification reactions.

Esterification Reaction

Preparation of long-chain organic acid cellulose esters in a Py/TsCl system followed the procedure discussed by Shimizu and Hayashi.[10,11] Fifteen grams of cellulose fibers were added to a 1-L five-necked flask containing a solution of 450 g of Py and 105 g of TsCl, with stirring and purging with nitrogen. Then, the carboxylic acid was slowly added into the mixture to give a 1 : 1 TsCl/acid molar ratio. The temperature of the reaction mixture was kept at 50°C in a temperature bath for 1(A) or 2 (B) h. After the reaction period, the fibers were filtered and washed with ethanol. All

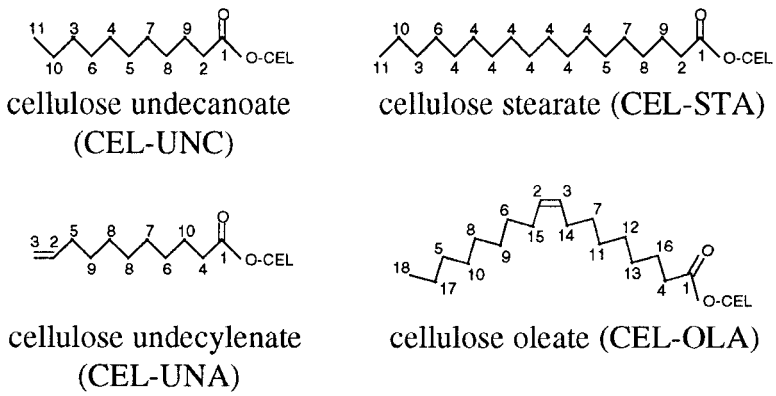

Figure 1 ^{13}C-NMR numeration of the carbon atoms in long-chain organic acid cellulose esters.

operations were performed under a fume hood due to escaping Py and ethanol vapor. After the fibers were Soxhlet-extracted with methanol for the first 2 h, the methanol was then changed for fresh methanol and the extraction continued for another 12 h. Finally, the fibers were filtered, washed with ethanol, dried with compressed air, and finally kept in a desiccator at room temperature for 20 h to evaporate the residual ethanol. The chemical formulas of CEL-EST are shown in Figure 1.

Degree of Substitution Determined by Gravimetry (DS_{Gr})

The degree of substitution (DS_{Gr}) determined by gravimetry was calculated using the formula

$$DS_{Gr} = \frac{GAIN \times MW_{AGU}}{100 \times (MW_{ACID} - MW_{OH})} \quad (1)$$

where *GAIN* [%] is the weight gain of cellulose fibers after the esterification reaction, $GAIN = [100\ m_3/(m_1 - m_2)] - 100$, where m_1 and m_3 are the weights [g] of cellulose fibers before and after the esterification reaction and m_2 is the weight loss of fibers after the reaction only with Py (all weights are calculated for an equivalent of 10 g of cellulose fibers); MW_{AGU}, the molecular weight of one anhydroglucose unit of cellulose (MW_{AGU} = 162 g/mol); MW_{ACID}, the molecular weight of an organic acid; and MW_{OH}, the molecular weight of one hydroxyl group (MW_{OH} = 17 g/mol).

FTIR–DRIFT Measurements

IR spectra were recorded using a Nicolet 510 P FTIR spectrometer with a diffuse reflectance accessory (DRIFT) and they are presented in the Kubelka–Munk absorbency mode. Resolution for all infrared spectra was 4 cm^{-1} with 40 scans. KBr was used as a reference material to produce a background diffuse reflectance spectrum.

Solid-state CP/MAS ^{13}C-NMR Measurements

Solid-state CP/MAS ^{13}C-NMR spectra were obtained at 75.3 MHz using a Chemagnetics CMX-300 spectrometer. Samples of dry fibers were placed in 7.5-mm zirconia rotors and spun at 4 kHz. The spectra were acquired using a variable-amplitude cross-polarization pulse sequence with 10 steps of the proton pulse amplitude, each lasting 300 μs, for a total contact time of 3 ms. (The application of a normal CP pulse sequence gave results for the degree of substitution which were only slightly less than were the results from the variable amplitude sequence.) The recycle delay was 1 s and 1000 transients were accumulated. High-power proton decoupling was carried out at 60 kHz.

Degree of Substitution Determined by ^{13}C-NMR (DS_{NMR})

The degree of substitution (DS_{NMR}) was calculated from a ratio of the integrals of NMR peaks[12] using the formula

$$DS_{NMR} = \frac{n_{CEL} \times I_{AC}}{n_{AC} \times I_{CEL}} \quad (2)$$

where I_{AC} and I_{CEL} are the integration of peaks of corresponding acyl carbons and cellulose carbons, respectively. n_{CEL} and n_{AC} are the number of

Table I Reaction Gain (*GAIN*) and Degree of Substitution (DS_{Gr}) Calculated by Gravimetry in Comparison with (DS_{NMR}) and Percent of Acyl Group (*AC*) Calculated from Solid-state CP/MAS ^{13}C-NMR Analysis in Cellulose Esters (CEL-EST)

		Gravimetry		^{13}C-NMR	
CEL-EST		*GAIN* (%)	DS_{Gr}	DS_{NMR}	*AC* (%)
CEL-UNA	A	46	0.44	0.47	32.6
	B	106	1.03	1.11	53.6
CEL-UNC	A	28	0.27	0.31	24.3
	B	61	0.58	0.59	38.2
CEL-OLA	A	20	0.12	0.08	11.4
	B	27	0.16	0.14	18.3
CEL-STA	A	21	0.13	0.12	17.1
	B	35	0.21	0.19	24.3

A = 1 h and B = 2 h reaction time.

carbon atoms in cellulose (n_{CEL} = 6) and in the corresponding acyl group.

The acyl content, AC [%], of CEL-EST was calculated using the Fordyce approach[13] using the formula

$$\mathrm{AC} = \frac{DS_{NMR}(MW_{ACID} - MW_{OH})}{MW_{AGU} + DS_{NMR}(MW_{ACID} - MW_{OH} - 1)} \times 100 \quad (3)$$

where DS_{NMR} is the degree of substitution of CEL-EST. The results are shown in Table I.

More spectra were run for each sample until consistent results were obtained with slight differences in DS_{NMR} to the second decimal place (about $\pm$0.02). The integration of spectra to obtain DS_{NMR} was performed without the deconvolution technique with the spectra plotted on an expanded scale in which small broad humps observed in the left halfs of some spectra shown in Figure 5 (background signal from equipment) are less obvious. The DS_{NMR} values would give reliable results rounded to the first decimal place. However, because of the lower degree of substitution in the case of CEL-OLA (0.08 and 0.14), it would be difficult to distinguish between the two samples, so the DS_{NMR} values rounded to the second decimal place are presented. Although the *DS* values calculated from both the gravimetry and NMR analyses are similar, the gravimetry calculations were not repeated, and, therefore, throughout the text, we refer to the *DS* values calculated from NMR data.

The NMR estimation of the dimensions of crystallites in the cellulose sample was based on a square cross-section cellulose crystallite model as shown in Figure 2 and described by Newman[14]:

$$L = \frac{2h}{1 - \sqrt{X}} \quad (4)$$

where L (nm) is the crystallite size, h = 0.57 nm is the thickness of the layer of surface chains, and X is the fraction of cellulose chains contained in the crystallite interior calculated from the areas of NMR C-4 peaks:

$$X = \frac{I_{C4}}{I_{C4} + I_{C4'}} \quad (5)$$

where I_{C4} is the integrated area of the C4 peak with its maximum at 89.4 ppm and $I_{C4'}$ is the area of its shoulder C4′ at 84.7 ppm.

X-ray Diffraction Measurements

The randomly oriented fibers were prepared into small pellets, 10 mm in diameter and 1–2 mm in thickness. X-ray diffraction spectra were recorded

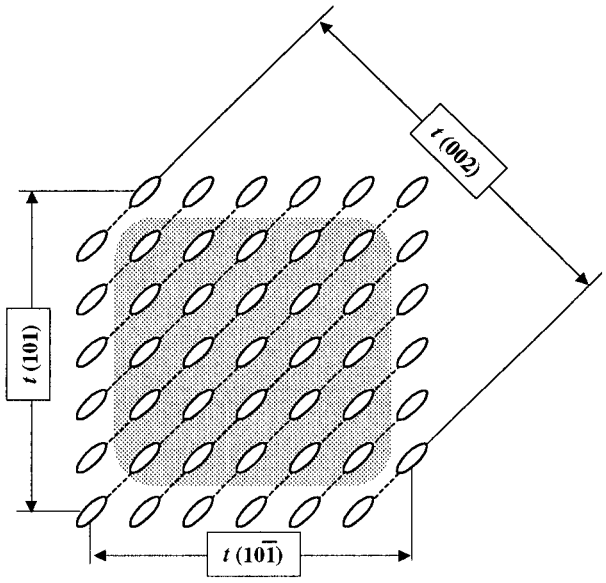

Figure 2 Model of a cross section through a cellulose crystallite. Each ellipse represents a glucose unit and dotted lines represent hydrogen bonds. Cellulose chains are oriented normal to the plane of the paper. The shadowed area shows the crystallite interior.

using a Siemens 500 D diffractometer equipped with CuKα radiation. The spectra were obtained at 190 mA with an accelerating voltage of 50 kV. Samples were scanned on the automated diffractometer from 5 to 40° of 2θ (Bragg angle). All recorded spectra were normalized at the same total scattering between 9 and 38° (2θ).

A peak resolution program was used to calculate the dimensions of crystallites in the cellulose sample (CEL) through peak broadening.[15] The spectrum was corrected for the background attributed to the amorphous region of the sample[16–18] simply by driving a straight line through the peak minima. The resolution of X-ray diffraction patterns yielded into Gauss–Lorentzian peaks, which represent the contribution of each of the diffraction planes. The apparent dimensions of cellulose crystallites were obtained by applying the Scherrer equation to the data of deconvoluted peaks:

$$t(hkl) = \frac{K\lambda}{B \cos \theta} \tag{6}$$

where t is the thickness of crystallites at the (hkl) plane of diffraction; λ, the wavelength of the X-ray source (λ = 1.5418 Å for CuKα); K, the Scherrer constant (K = 0.9); B, the peak full width at the half-maximum height, and θ, the Bragg angle for the (hkl) plane.

RESULTS AND DISCUSSION

FTIR–DRIFT

IR spectra of CEL-UNA and CEL-UNC are shown in Figure 3, and CEL-OLA and CEL-STA, in Figure 4, together with original cellulose fibers. The spectra of organic acids were taken from the literature and represent gas-phase absorption infrared spectra.[19]

All CEL-EST spectra have a common absorption in ester carbonyl stretching C═O with its frequency increasing with a higher *DS* (exact values are as follows: 1748 cm^{-1} CEL-UNA-A, 1751 cm^{-1} CEL-UNA-B, 1746 cm^{-1} CEL-UNC-A, 1746 cm^{-1} CEL-UNC-B, 1744 cm^{-1} CEL-OLA-A, 1743 cm^{-1} CEL-OLA-B, 1745 cm^{-1} CEL-STA-A, 1746 cm^{-1} CEL-STA-B). These findings are similar to those published by Warwicker and Spedding[3] for cellulose acetates with different *DS* and to results obtained on highly substituted cellulose derivatives.[20] The changes in carbonyl frequencies suggest a weakening of hydrogen bonds between ester carbonyl groups and the remaining cellulose hydroxyl groups. For comparison, the carbonyl stretching of gas IR of organic acids[19] are shifted to higher wavenumbers (1761 cm^{-1} UNA, 1779 cm^{-1} UNC, OLA, and STA).

Asymmetric and symmetric CH_2 stretching are at 2926 and 2856 cm^{-1}, respectively, arising from the aliphatic chain of an organic acid. Cellulose in this region has a broad band of CH stretching at 2902 cm^{-1}.

A lower intensity of broad the cellulose hydroxyl absorption peak at about 3400 cm^{-1} is shown with an increased *DS* in the CEL-EST. There are two new peaks in the cellulose hydroxyl region arising at 3474 and 3355 cm^{-1} in the case of CEL-UNC and more apparent in CEL-UNA as shown in Figure 3. The frequency of hydrogen-bonded OH groups depends partly upon whether the oxygen atoms also act as a proton acceptor for another group. Marrinan and Mann[21] discussed that these peak shifts are due to hydroxyl groups participating in O—H · · · O for the former (3474 cm^{-1}) and the groups participating in two hydrogen bonds of the type H · · · O—H · · · O for the latter (3355 cm^{-1}). Hydroxyl groups of organic acids measured by gas IR have their peaks at a higher frequency (3587 cm^{-1}). These findings described above indicate that, in the case of CEL-UNA-B, the hydroxyl groups in less-ordered regions of cellulose were substituted with an organic acid and that two new OH peaks arising from the microfibril's ordered regions are now dominant in this part of the IR spectra.

Unsaturation is observed in CEL-UNA at 1641 cm^{-1} arising from C═C stretching in the UNA chain. Also, there are two peaks of C—H stretching at 3077 cm^{-1} and C—H bending at 910 cm^{-1} arising from a —CH═CH_2 group in *trans* conformation.[22] It is interesting to point out that these absorption peaks are not present in UNA.

The C═C stretching vibration band is not observed in CEL-OLA because it is very weak when it is internal in symmetrical molecules in *cis* conformation (in the case of oleic acid) and is not observed in oleic acid also because there is interfering absorption from the strong C═O stretching vibration.[22]

All CEL-EST infrared spectra show increasing intensities of two bands, first at 1166-cm^{-1} cellulose antisymmetric bridge oxygen stretching and C—O stretching at 1065 cm^{-1}. Together with antisymmetric in-phase cellulose ring wagging at

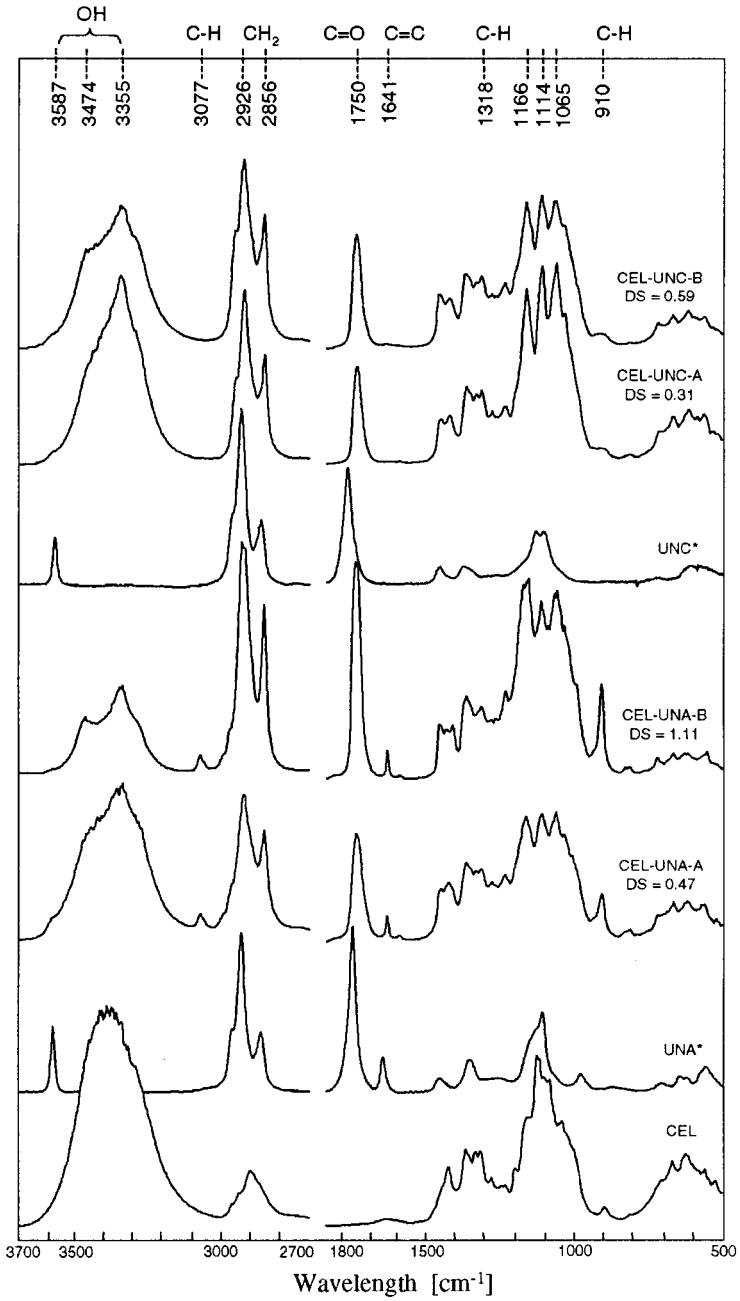

Figure 3 Diffuse reflectance infrared spectra of cellulose, cellulose esters CEL-EST-11, and corresponding organic acids. *Gas-phase absorption infrared spectra taken from the literature.[19]

1114 cm^{-1}, they are shown as a characteristic three peaks.

The reflectance IR spectra demonstrated the chemical substitution of hydroxyl groups with organic acids. Clear evidence for the esterification reaction was observed by the appearance of a new ester carbonyl band and an increased intensity of CH_2 stretching arising from an organic acid chain. On the other hand, the decrease and the sharpening of a broad peak in the cellulose hydroxyl region suggested the disappearance of intensities originated from hydroxyls in less ordered regions due to their substitution with an organic acid and revealed the remaining hydroxyl groups from crystalline regions. In the case of CEL-EST-11, the possibility of the involvement of

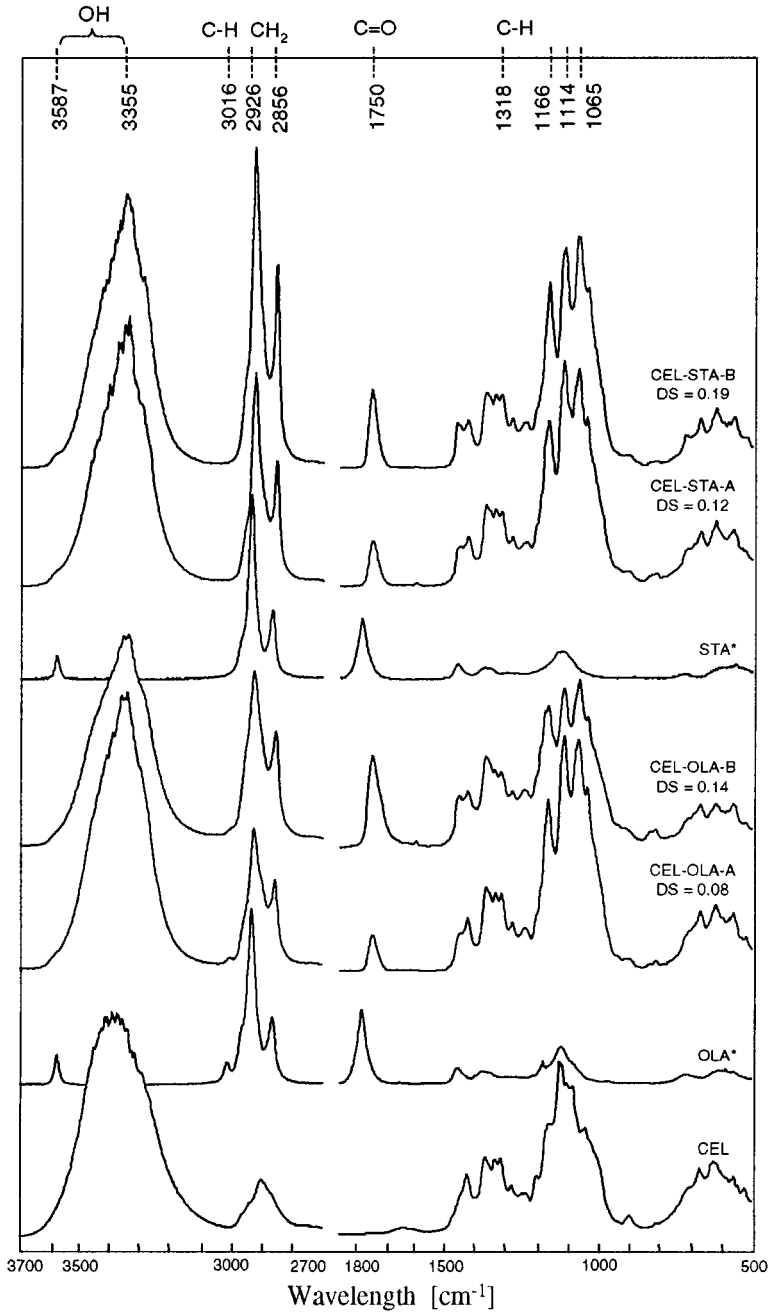

Figure 4 Diffuse reflectance infrared spectra of cellulose, cellulose esters CEL-EST-18, and corresponding organic acids. *Gas-phase absorption infrared spectra taken from the literature.[19]

cellulose crystallites regions in the chemical reaction was considered.

Solid-State CP/MAS ^{13}C-NMR

Solid-state ^{13}C-NMR spectra of the original cellulose sample and cellulose esters synthesized after 2 h of esterification (resonance shifts of CEL-EST acyl carbons are independent of *DS*) are presented in Figure 5. Peak assignment of acyl carbons was made according to the literature.[23] Organic acid carbonyl carbons are strongly deshielded by electronegative oxygen atoms and have their resonance peaks between 180.6 and 180.8 ppm.[23] The resonance of carbonyl groups in

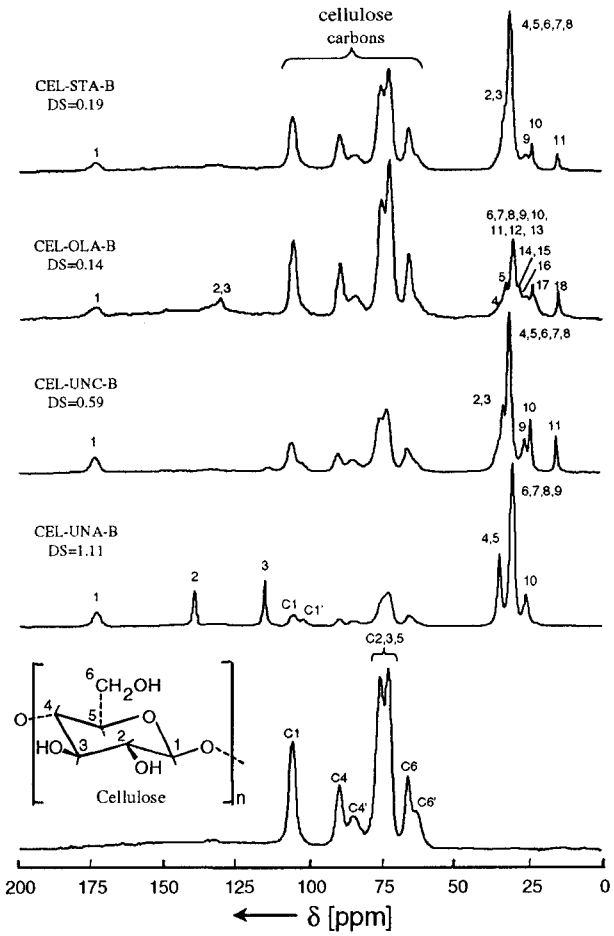

Figure 5 CP/MAS ^{13}C-NMR spectra of cellulose and long-chain organic acid cellulose esters after a 2-h esterification reaction.

CEL-EST is upfield-shifted and appears at 173.5–173.7 ppm, suggesting that the esterification reaction took place.

The ratio obtained from corresponding integration in the spectra, which is 5.1 : 1, is similar to the theoretical ratio between the number of carbon atoms in the anhydroglucose unit C-2,3,4,5,6/C-1, which is 5 : 1. For comparison purposes, cellulose carbon peaks were normalized for C-4 peak intensities ($I_{C4} + I_{C4'} = 1$). The intensities of the carbonyl peaks obtained after normalization are in linear correlation with an increasing *DS* of CEL-EST as shown in Figure 6.

The assignment of cellulose carbon peaks is well documented in the literature[24–28]; however, only a few articles on solid-state CP/MAS ^{13}C-NMR spectra of esterified cellulose have been published. These studies compared solution and solid-state ^{13}C NMR spectra of heterogeneously acetylated cellulose as a function of degree of substitution,[5] several cellulose derivatives including cellulose triacetate, tripropionate, tributyrate, and trinitrate, and some cellulose ethers,[29] long-chain fatty acid cellulose ester synthesized with soybean oil,[7] cellulose acetate and cellulose propionate as powder,[30] or cellulose triacetate and its oligomers ($DP = 2–9$).[31]

The explanation of peak broadness in solid-state CP/MAS ^{13}C-NMR for cellulose fibers in earlier studies suggests that crystalline regions of cellulose give a narrow resonance, while noncrystalline or paracrystalline regions give a broader resonance.[26] The broadness in the resonance of noncrystalline regions is due to a greater disorder in molecular packing, distribution of molecular conformations, and/or higher molecular mobility in these regions.[25]

There is more evidence that a narrow C4 peak can be associated with cellulose chains contained within crystals and a broader C4′ shoulder with chains exposed on crystallite surfaces.[14,24,25,28,32] The chemical-shift difference between these two bands is attributed to a difference in patterns of hydrogen bonding. Each cellulose chain in the crystallite interior is hydrogen-bonded to its two neighboring chains (cellulose-I model). On a crystallite surface, however, the cellulose chain is hydrogen-bonded to just one adjacent chain of the crystallite interior.

A detailed series of normalized NMR spectra in the region of cellulose carbons for the cellulose sample and all cellulose esters (CEL-EST-11 and CEL-EST-18) is shown in Figure 7. The signal at 105.6 ppm due to C-1 carbon shows one peak for the CEL sample and de-

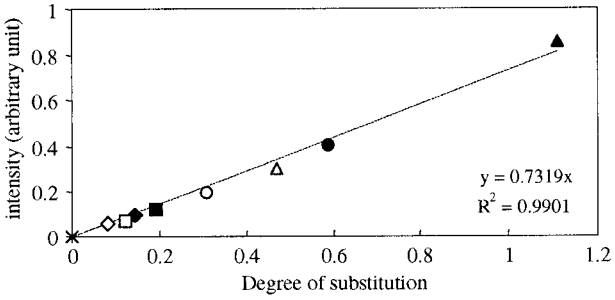

Figure 6 Normalized CP/MAS ^{13}C-NMR carbonyl integral intensities versus degree of substitution of cellulose esters: (×) CEL; (△) CEL-UNA-A, $DS = 0.47$; (▲) CEL-UNA-B, $DS = 1.11$; (○) CEL-UNC-A, $DS = 0.31$; (●) CEL-UNC-B, $DS = 0.59$; (◇) CEL-OLA-A, $DS = 0.08$; (◆) CEL-OLA-B, $DS = 0.14$; (□) CEL-STA-A, $DS = 0.12$; (■) CEL-STA-B, $DS = 0.19$.

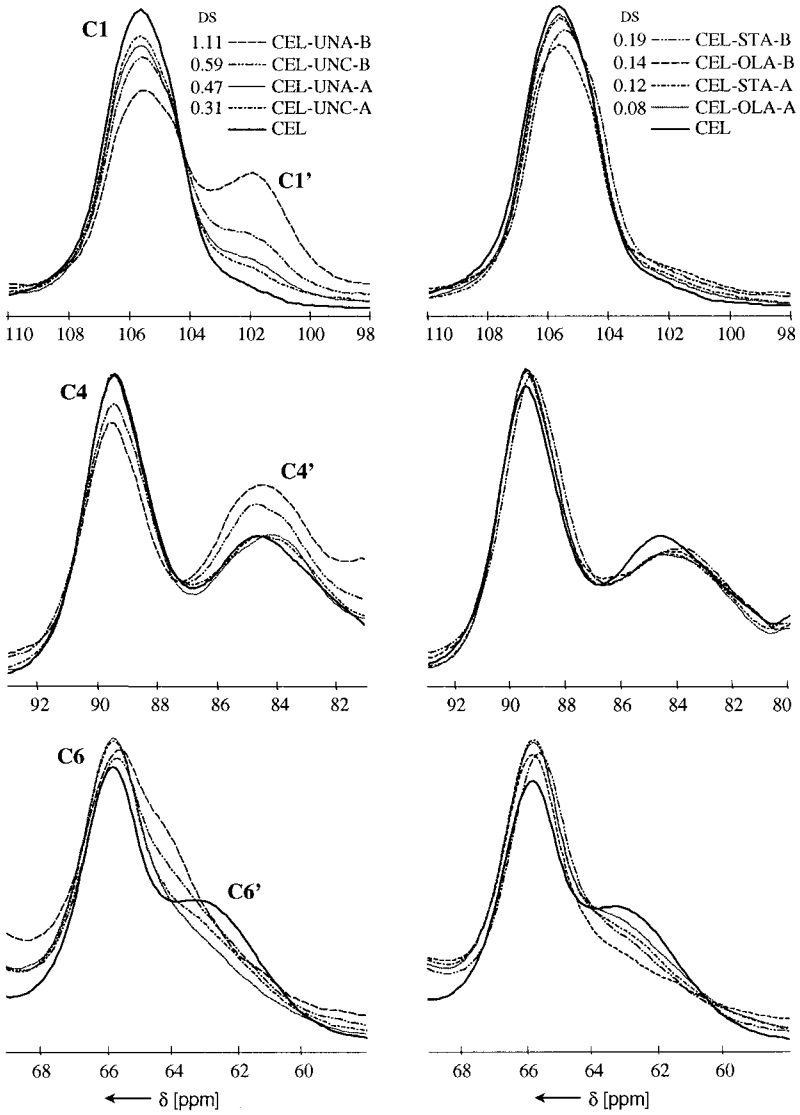

Figure 7 CP/MAS ^{13}C-NMR detailed spectra of cellulose anhydroglucose carbons in cellulose esters.

creases gradually in CEL-EST as the *DS* increases. In the case of CEL-EST-11, a new band assigned as C1′ arises with its maximum at 101.9 for CEL-UNA-B (*DS* = 1.11). This effect is less intense in the case of CEL-EST-18.

C-4 carbons in CEL show a splitting as a narrow C4 peak at 89.4 and a broader C4′ peak at 84.7 ppm. Some interesting observations may be made: In the case of CEL-EST-11, the narrow C4 peak decreases and the broader C4′ increases after 2 h of esterification in the case of CEL-UNC-B (*DS* = 0.59) and CEL-UNA-B (*DS* = 1.11). This would lead to the conclusion that the dimensions of crystallites was affected during the esterification reaction if the assignment of C4/C4′ regions represents the crystallites interior/surface chains, as discussed before. However, to make a quantitative conclusion is more complicated because the intensities of cellulose carbon atoms carrying substituted hydroxyl groups should also be present in the C4′ region of the spectrum and therefore influencing the C4/C4′ intensity ratio. Such derived dimensions of crystallites would be, hence, underestimated. The new unassigned peak in the C-4 region of substituted cellulose chains is not seen from the spectra, probably due to low NMR resolution.

Wickholm et al.[33] calculated the lateral fibril dimensions of cellulose samples after an acid hy-

drolysis procedure which removed the interfering signals found in the C4′ region originating from hemicelluloses. Another approach was used by Newman[14] where the NMR spectra were separated into signals assigned to cellulose crystallites and signals assigned to amorphous material. The lateral dimensions of crystallites in several solid lignocellulosics calculated from ^{13}C NMR and from X-ray scattering data were compared. It was found that those estimated by X-ray were about 10% lower than were those estimated by NMR.

In this work, the dimensions of crystallites in the only cellulose sample (CEL) were calculated using a square cross-section crystallite model shown in Figure 2, with spacing between chains of 0.57 nm, described by Newman.[14] The model represents the fraction of cellulose chains in the crystallites interior (0.53) close to the value $X = 0.57$ calculated through eq. (5) from data of the fitted C-4 region of the NMR spectra. The size of cellulose crystallites calculated with eq. (4) was $L = 4.6$ nm.

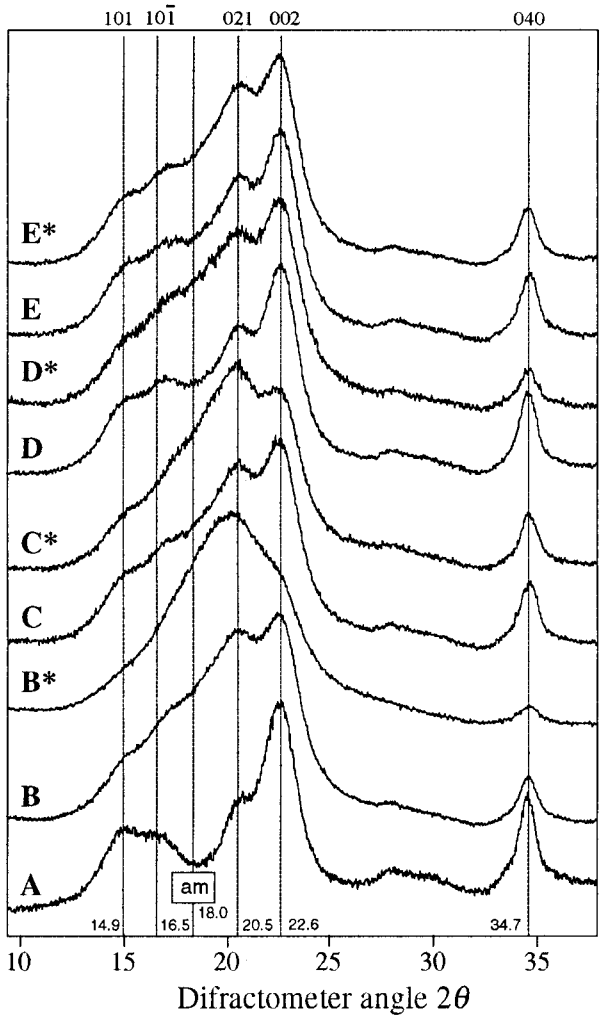

Figure 8 X-ray diffraction spectra of cellulose and cellulose esters: (A) Cellulose; (B) CEL-UNA-A, $DS = 0.47$; (B*) CEL-UNA-B, $DS = 1.11$, (C) CEL-UNC-A, $DS = 0.31$; (C*) CEL-UNC-B, $DS = 0.59$; (D) CEL-OLA-A, $DS = 0.08$; (D*) CEL-OLA-B, $DS = 0.14$; (E) CEL-STA-A, $DS = 0.12$; (E*) CEL-STA-B, $DS = 0.19$. am, intensity of amorphous regions of cellulose.

When cellulose was esterified with organic acids with 18 carbon atoms (CEL-EST-18), these changes were smaller but reversed. The C4 peak increased and C4′ decreased. In this case, the new rearrangement of cellulose chains in the less-ordered region could lead to this effect, probably resulting in a small increase of the crystallinity in the samples, but it was not confirmed by the X-ray analysis.

The two overlapping peaks at 75.3 and 72.6 ppm in Figure 5 are C-2, C-3, and C-5 carbons. Until now, these peaks have not been assigned to specific carbons.

The C-6 carbons have two overlapping peaks: a narrow C6 at 65.8 ppm and its upfield shoulder C6′ at 63.3 ppm. In both CEL-EST-11 and CEL-EST-18, the upfield shoulder C6′ tends to disappear and the narrow C6 peak increases with higher *DS* of CEL-EST. C6′ in CEL-EST-11 is probably shifted downfield as the C6 carbon atoms become less mobile after the substitution of C6-hydroxyls with an organic acid.

A comparison of NMR spectra indicates that significant variations of intensity occur in the region of the C-1, C-4, and C-6 peaks as a function of the *DS*. However, due to the low resolution of the NMR spectra and the lack of information about the assignment of new intensities to the substituted cellulose carbons in the C-4 region, it was not possible to calculate the dimensional changes of cellulose crystallites after the esterification. These changes in the NMR spectra are more evident in CEL-EST-11 and follow the same trend as observed by Doyle et al.[5] on heterogeneously acetylated cellulose.

X-ray Diffraction

Diffraction patterns obtained from CEL and CEL-EST samples are shown in Figure 8. The progressive decrease and broadening of intensities connected with the 101, 10$\bar{1}$, and 002 planes and decrease of intensity of 040 planes can be observed. On the other hand, there is an increase of diffraction intensities in the amorphous region of

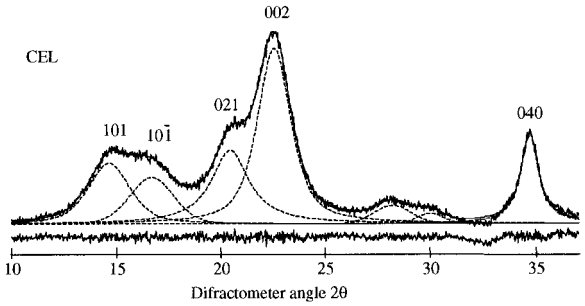

Figure 9 Resolution of X-ray diffraction pattern of cellulose sample (CEL).

cellulose at around 18° which is attributed to the less-ordered region of cellulose chains.[34] X-ray diffraction studies on cellulose acetates showed that the heterogeneous acetylation process leads to an increase in the amorphous content of the material and the generation of a crystalline peak associated with cellulose triacetate near the amorphous region of cellulose.[35,36] Until now, there were no studies with X-ray diffraction to determine whether cellulose chains substituted with long-chain organic acids in a heterogeneous esterification reaction form an ordered structure. The lack of information about the morphology of such cellulose esters complicates the estimation of the dimensions of cellulose crystallites. Therefore, only an original cellulose sample (CEL) was used to calculate the dimensions of crystallites from X-ray data obtained from the fitted spectra shown in Figure 9. The value calculated using eq. (6) for the 002 plane was $t = 4.1$ nm, which, in comparison with $L = 4.6$ nm derived from NMR data, shows a difference of about 11%. This is in agreement with the observations made by Newman[14] as discussed earlier.

X-ray diffraction spectra of cellulose esters show broader peaks at angles slightly different from those for cellulose. The origin of these broad peaks may come from a smaller size of cellulose crystallites as the esterification reaction continues. However, one has to consider also an amorphous region of disordered cellulose chains, or an amorphous ester at 18°, or perhaps a new well-ordered ester, all appearing at angles around 18°–20°.

CONCLUSIONS

In this study, several analytical techniques were used to characterize chemical and morphological changes of cellulose fibers after an esterification reaction with long-chain organic acids. Diffuse reflectance infrared spectroscopy (DRIFT) provides evidence of a substitution reaction and suggests changes in the dimensions of cellulose crystallites in the case of CEL-EST-11. The solid-state CP/MAS ^{13}C-NMR and X-ray diffraction spectra support the view about morphological changes and suggests considering more categories of different lateral order in substituted fibers.

The authors would like to thank Dr. Fred Morin in the Chemistry Department of McGill University for recording the solid-state CP/MAS ^{13}C-NMR spectra, Mr. Luc Lévesque and Dr. Josée Brisson from Laval University in Quebec for taking the X-ray diffraction spectra, and all of them for their helpful discussions. The authors would also like to thank Dr. Tomas Larsson from the Swedish Pulp and Paper Research Institute and Dr. Roger Newman from Industrial Research in New Zealand for helpful discussions about NMR spectra. The authors gratefully acknowledge the financial support of the Natural Science and Engineering Research Council (NSERC), Canada.

REFERENCES

1. Stipanovic, A. J.; Sarko, A. Polymer 1978, 19, 3–9.
2. Crofton, D. J.; Doyle, S.; Pethrick, R. A. In Cellulose and Its Derivatives: Chemistry, Biochemistry, and Applications; Kennedy, J. F.; Phillips, G. O.; Wedlock, D. J.; Williams, P. A., Eds.; E. Horwood: Chichester (West Sussex); Halsted: New York, 1985.
3. Warwicker, J. O.; Spedding, H. J Appl Polym Sci 1965, 9, 1913–1928.
4. Battista, O. A.; Armstrong, A. T.; Radchenko, S. S. Polym Prepr Am Chem Soc Div Polym Chem 1978, 19, 567–571.
5. Doyle, S.; Pethrick, R. A.; Harris, R. K.; Lane, J. M.; Packer, K. J.; Heatley, F. Polymer 1986, 27, 19–24.
6. Malm, C. J.; Mench, J. W.; Kendall, D. L.; Hiatt, G. D. Ind Eng Chem 1951, 43, 688–691.
7. Wang, P.; Tao, B. Y. J Appl Polym Sci 1994, 52, 755–776.
8. Sealey, J. E.; Samaranayake, G.; Todd, J. G.; Glasser, W. G. J Polym Sci Part B Polym Phys 1996, 34, 1613–1620.
9. Hudson, S. H.; Cuculo, J. A. J Macromol Sci Rev Macromol Chem 1980, 18, 1–82.
10. Shimizu, Y.; Hayashi, J. Sen-I Gakkaishi 1988, 44, 451–456.
11. Shimizu, Y.; Hayashi, J. Cell Chem Technol 1989, 23, 661–670.

12. Raymond, L.; Morin, F. G.; Marchessault, R. H. Carbohydr Res 1993, 246, 331–336.
13. Fordyce, C. R.; Genung, L. B.; Pile, M. A. Ind Eng Chem Anal Ed 1946, 18, 547–550.
14. Newman, R. H. Solid State Nucl Magn Reson 1999, 15, 21–29.
15. Bartram, S. F. In Handbook of X-ray; Kaelble, E. F., Ed.; McGraw-Hill: New York, 1967; Chapter 17.
16. Hermans, P. H.; Weidinger, A. J Appl Phys 1948, 19, 491–506.
17. Hindeleh, A. M.; Johnson, D. J. Polymer 1978, 19, 27–32.
18. Ramos, L. P.; Nazhad, M. M.; Sadler, J. N. Enzyme Microb Technol 1993, 15, 821–831.
19. The National Institute of Standards and Technology (NIST) Standard Reference Database 69, Nov. 1998.
20. Jeffries, R. Polymer 1963, 4, 375–389.
21. Marrinan, H. J.; Mann, J. J Appl Chem 1954, 4, 204–211.
22. O'Connor, R. T. In Fatty Acids; Markley, K. S.; Krieger, R. E. Eds.; Malabar, FL, 1983, pp 379–498.
23. The Aldrich Library of ^{13}C and 'H FTNMR Spectra, ed. 1; Puochert, C. J.; Behnke, J., Eds.; Aldrich Chemical Co.: Milwaukee, WI, 1993, Vol. 1.
24. Earl, W. L.; VanderHart, D. L. J Am Chem Soc 1980, 102, 3251–3252.
25. Earl, W. L.; VanderHart, D. L. Macromolecules 1981, 14, 570–574.
26. Horii, F.; Hirai, A.; Kitamaru, R. Polym Bull 1982, 8, 163–170.
27. Horii, F.; Hirai, A.; Kitamaru, R.; Sakurada, I. Cell Chem Technol 1985, 19, 513–523.
28. Newman, R. H.; Ha, M.; Melton, L. D. J Agric Food Chem 1994, 42, 1402–1406.
29. Hoshino, M.; Takai, M.; Fukuda, K.; Imura, K.; Hayashi, J. J Polym Sci Part A Polym Chem 1989, 27, 2083–2092.
30. Nunes, T.; Burrowst, H. D.; Bastos, M.; Feio, G.; Gil, M. H. Polymer 1995, 36, 479–485.
31. VanderHart, D. L.; Hyatt, J. A.; Atalla, R. H.; Tirumalai, V. C. Macromolecules 1996, 29, 730–739.
32. Newman, R. H. Holzforschung 1998, 52, 157–159.
33. Wickholm, K.; Larsson, P. T.; Iversen, T. Carbohydr Res 1998, 312, 123–129.
34. Segal, L.; Creely, J. J.; Martin, A. E., Jr.; Conrad, C. M. Text Res J 1959, 29, 786–794.
35. Takai, M.; Fakuda, K.; Murata, M.; Hayashi, J. In Wood and Cellulosics; Kennedy, J. F.; Phillips, G. O.; Williams, P. A., Eds.; Ellis Horwood: Chichester, 1987; pp 111–117, Chapter 12.
36. Doyle, S. E.; Gibbons, A. M.; Pethrick, R. A. In Wood and Cellulosics; Kennedy, J. F.; Phillips, G. O.; Williams, P. A., Eds.; Ellis Horwood: Chichester, 1987; pp 71–76, Chapter 7.